ChemComm

COMMUNICATION

View Article Online
View Journal | View Issue

Cite this: *Chem. Commun.*, 2021, **57**, 7541

Received 24th April 2021,
Accepted 16th June 2021

DOI: 10.1039/d1cc02173g

rsc.li/chemcomm

Higher MLCT lifetime of carbene iron(II) complexes by chelate ring expansion†

Thomas Reuter,[a] Ayla Kruse,[b] Roland Schoch,[c] Stefan Lochbrunner,[b] Matthias Bauer[c] and Katja Heinze *[a]

Combining strong σ-donating N-heterocyclic carbene ligands and π-accepting pyridine ligands with a high octahedricity in rigid iron(II) complexes increases the ^{3}MLCT lifetime from 0.15 ps in the prototypical $[Fe(tpy)_2]^{2+}$ complex to 9.2 ps in $[Fe(dpmi)_2]^{2+}$ $\mathbf{1}^{2+}$. The tripodal CNN ligand dpmi (di(pyridine-2-yl)(3-methylimidazol-2-yl)methane) forms six-membered chelate rings with the iron(II) centre leading to close to 90° bite angles and enhanced iron-ligand orbital overlap.

Replacing expensive ruthenium(II) and iridium(III) complexes possessing long-lived metal-to-ligand charge transfer (MLCT) states in photochemical or photophysical applications with cheaper and more abundant alternatives is a highly important yet very challenging objective for future large-scale implementation.[1–4] Iron(II) complexes, isoelectronic to Ru^{II} and Ir^{III} have found tremendous interest for these purposes.[5–8] However, due to a much smaller ligand field splitting,[9] Fe^{II} complexes possess low-energy metal-centred states (^{3}MC and ^{5}MC) which provide efficient non-radiative relaxation pathways. Consequently, the MLCT photochemistry of iron(II) complexes is much less developed than for the classical ruthenium(II) or iridium(III) complexes.[10,11] Concepts to prolong the lifetime of the potentially emissive ^{3}MLCT state aim to increase the energy of the MC states and to decrease the energy of ^{3}MLCT states.[5–7]

The latter has been targeted by using electron-poor π-accepting ligands[12–15] while the energy of the MC states has been increased using a better metal–ligand orbital overlap in highly octahedral polypyridyl complexes with N–M–N angles close to 180°[12–14] or strong σ-donating carbene ligands.[6,7,15–20] The concept of large bite angles to separate ^{3}MLCT from MC states had been very successful in the photophysical optimisation of ruthenium(II) sensitizers and phosphorescent emitters.[21–25] In structurally related carbene pyridine iron(II) complexes with tridentate ligands forming five-membered chelate rings, the number of carbene donors dictates the ^{3}MLCT lifetime.[17] The highest lifetime (528 ps) of carbene iron(II) complexes has been achieved with six carbene donors in $[Fe(btz)_3]^{2+}$ (btz = 3,3'-dimethyl-1,1'-bis(*p*-tolyl))-4,4'-bis(1,2,3-triazol-5-ylidene).[20] The effect of six-membered chelate rings to increase the metal ligand orbital overlap and consequently the energy of MC states of 3d metal complexes has been demonstrated with polypyridyl vanadium(III) and chromium(III) complexes[26–28] as well as hexacarbene manganese(IV) and iron(III) complexes,[29,30] while polypyridyl iron(II) complexes with high octahedricity still feature low MLCT lifetimes. The combination of four carbenes with six-membered chelate rings in iron(II) complexes with tridentate meridionally coordinating CNC ligands only provided low MLCT lifetimes of around 1 ps of the majority of the excited state population which has been ascribed to a higher flexibility of this CNC ligand.[31]

Here, we combine high octahedricity with π-accepting pyridine and σ-donating carbene ligands in a more rigid coordination environment to increase the ^{3}MLCT lifetime of iron(II) complexes. We compare the $[C_2N_4]$ donor set in the novel more octahedral carbene iron(II) complex $[Fe(dpmi)_2]^{2+}$ $\mathbf{1}^{2+}$ (Scheme 1) featuring facially coordinating dpmi ligands (di(pyridine-2-yl)(3-methylimidazol-2-yl)methane) that form six-membered chelate rings with distorted $[Fe(CNC)_2]^{2+}$ and $[Fe(CNN)_2]^{2+}$ complexes possessing five-membered chelate rings in terms of the resulting ^{3}MLCT lifetime. The distorted $[Fe(CNC)_2]^{2+}$ and $[Fe(CNN)_2]^{2+}$ complexes with five-membered rings exhibit ^{3}MLCT lifetimes below 0.1 ps.[17] We demonstrate that the more octahedral and rigid complex geometry increases the lifetime even beyond that of a $[C_4N_2]$ donor set in distorted carbene pyridine iron(II) complexes (τ = 9, 8.1, <0.3 ps for $[Fe(CNC)_2]^{2+}$ with Me, ^{i}Pr, ^{t}Bu N-substituents).[16,17] Consequently, the higher octahedricity and rigidity of $\mathbf{1}^{2+}$ has a similar boosting effect as two strong carbene σ-donors in distorted $[Fe(CNC)_2]^{2+}$ complexes.

[a] *Department of Chemistry, Johannes Gutenberg University of Mainz, Duesbergweg 10-14, Mainz 55128, Germany. E-mail: katja.heinze@uni-mainz.de*
[b] *Institute for Physics and Department of Life, Light and Matter, University of Rostock, Rostock 18051, Germany*
[c] *Faculty of Science, Chemistry Department and Centre for Sustainable Systems Design, Paderborn University, Paderborn 33098, Germany*

† Electronic supplementary information (ESI) available: General procedures, synthesis, spectral data, computational data. See DOI: 10.1039/d1cc02173g

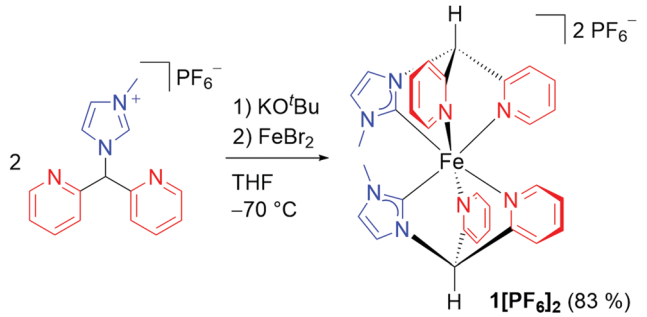

Scheme 1 Synthesis of **1[PF6]$_2$** starting from the pro-ligand [Py$_2$MeImH][PF$_6$].[32]

The tridentate facially coordinating CNN ligand derived from [Py$_2$MeImH][PF$_6$][32] after deprotonation forms six-membered chelate rings with iron(II) in the homoleptic complex cation **1**$^{2+}$ (Scheme 1). Complex **1**$^{2+}$ with a [C$_2$N$_4$] donor set was characterised by IR, NMR spectroscopy, ESI$^+$ mass spectrometry and elemental analysis (ESI). The 12 and 15 ^{1}H and ^{13}C NMR resonances observed (ESI) are consistent with a *cis* configuration of the carbene donors and the expected destabilising *trans* influence in a conceivable *trans* configuration. Six Fe–C/N atom distances of 1.99(8) Å were determined by iron K-edge EXAFS of **1[PF6]$_2$** (ESI). Four Fe···N distances of 2.79(4) Å fit to the four NHC nitrogen atoms. The averaged Fe–C/N distances obtained by the EXAFS experiment agree with a structural model derived from quantum chemical calculations of low-spin **1**$^{2+}$ (DFT CPCM(acetonitrile)-RIJCOSX-B3LYP-D3BJ-ZORA/def2-TZVP; averaged Fe–C/N distance of 1.999 Å and averaged Fe···N$_{carbene}$ distances of 2.943 Å; ESI). The pre-edge peak at 7113.3 eV in the iron K-edge X-ray absorption spectrum[33] and the NMR data of **1[PF$_6$]$_2$** confirm the low-spin state of the iron(II) centre. The energies of the pre-peak and the near-edge shoulders around 7120 and 7123 eV of **1**$^{2+}$ (ESI) are essentially identical to that of a [Fe(CNN)$_2$]$^{2+}$ complex with *cis*-positioned carbene donors in a more distorted geometry (7113.3, 7120, 7123 eV).[17]

The electronic absorption spectrum of **1**$^{2+}$ in acetonitrile shows two absorption bands at 415 nm (ε = 17310 L mol^{-1} cm^{-1}) and 500 nm (ε = 19390 L mol^{-1} cm^{-1}) (Fig. 1a). Their intensities agree with allowed charge transfer transitions and exceed those of other carbene and pyridine iron(II) complexes, *e.g.* 700 nm (2000 L mol^{-1} cm^{-1}), 508/557 nm (4700/7000 L mol^{-1} cm^{-1}), 503/538 nm (9800/8600 L mol^{-1} cm^{-1}) and 551 nm (7000 L mol^{-1} cm^{-1}) for [Fe(btz)$_3$]$^{2+}$,[20] [Fe(CNN)$_2$]$^{2+}$, [Fe(CNC)(tpy)]$^{2+}$ and [Fe(tpy)$_2$]$^{2+}$, respectively.[17] According to time-dependent DFT (TDDFT) calculation and charge transfer number analysis,[34] these two intense bands consist of $d_{Fe} \rightarrow \pi_{pyridine}$ ^{1}MLCT transitions, while $d_{Fe} \rightarrow \pi_{carbene}$ ^{1}MLCT transitions appear at higher energy (ESI). Less allowed transitions are calculated at lower energy. The charge transfer number analysis assigns mainly ^{1}MC character to these bands, suggesting that ^{1}MC states are lower in energy than ^{1}MLCT states.

The iron(II) complex **1**$^{2+}$ is reversibly oxidised to **1**$^{3+}$ at $E_{1/2}$ = 0.26 V *vs.* ferrocene in the cyclic voltammogram (MeCN, [^{n}Bu$_4$N][PF$_6$], ESI). Spectro-electrochemical oxidation of **1**$^{2+}$ to **1**$^{3+}$

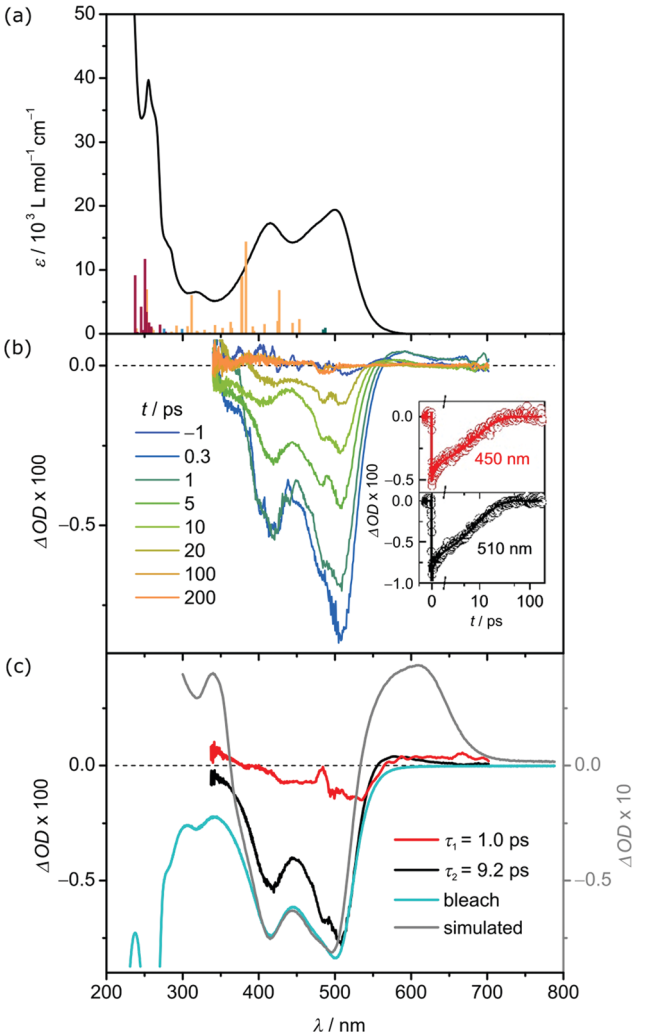

Fig. 1 (a) UV/Vis absorption spectrum of **1[PF$_6$]$_2$** (black) in deaerated acetonitrile and TDDFT calculated transitions of **1**$^{2+}$ with the colour code indicating the character of the transition according to charge transfer analysis (dark green: MC, orange: MLCT, dark red: LL'CT). (b) Transient absorption spectra of **1[PF$_6$]$_2$** in deaerated acetonitrile at selected time points from 0.3 to 200 ps after excitation at 490 nm. The insets show time traces probed at 450 nm (red) and 510 nm (black) and corresponding fits. (c) Decay associated amplitude spectra (DAS) of the 1.0 ps (red) and 9.2 ps (black) decay component compared to the scaled bleach (blue) and the difference spectrum[35] between **1**$^{3+}$ and **1**$^{2+}$ (grey).

bleaches the MLCT absorption bands while two new bands appear at 522 and 610 nm (ESI). These are ascribed to carbene/pyridine-to-iron charge transfer transitions (LMCT). Isosbestic points form at 253, 267, 356 and 544 nm confirming the reversible nature of the oxidation process. Chemical oxidation of orange **1**$^{2+}$ to blue **1**$^{3+}$ using [NO][PF$_6$] as oxidant is successful as well as supported by an identical UV/Vis spectral pattern (ESI).

Transient absorption (TA) spectroscopy on **1[PF6]$_2$** in deaerated MeCN discloses the excited state dynamics after excitation at 490 nm (MLCT). Fig. 1b shows the TA spectra recorded at selected time delays following excitation at 490 nm. The TA spectra display two negative bands at 420 and 505 nm, which correspond to the ground state bleach (GSB), and a weaker

excited state absorption (ESA) at approximately 560 nm. All signals decay on the 10 ps time scale (Fig. 1b, insets).

The dynamics is analysed by applying a global, triple-exponential fit, yielding a dominant decay component with a time constant of τ_2 = 9.2 ps and a weaker one of τ_1 = 1.0 ps. The third contribution exhibits a lifetime of only a few femtoseconds, which is much shorter than the actual time resolution, and resembles an artefact at time zero due to cross phase modulation. Fig. 1c compares the decay associated amplitude spectra (DAS) of the two relevant components τ_1 and τ_2 to the scaled bleach and the difference spectrum between $\mathbf{1}^{3+}$ and $\mathbf{1}^{2+}$. The DAS of the dominant τ_2 = 9.2 ps component is quite similar to the bleach but exhibits additional ESA contributions in the wavelength range 550–650 nm. The difference spectrum indicates that oxidation of iron(II) to iron(III) causes such an additional absorption. Below 400 nm the TA signal approaches zero with decreasing wavelength in contrast to the bleach pointing also there to an additional ESA contribution. This too, would be in line with an oxidation of the iron center. Accordingly, the 9.2 ps component describes the decay of a state involving iron(III) suggesting that it is the MLCT state.[30] The absorption band of $\mathbf{1}^{3+}$ at 610 nm and consequently the ESA of $\mathbf{1}^{2+}$ are of ligand→iron(III) LMCT character. The DAS of the 1.0 ps component is weak and exhibits a shape, which has some similarities with the dominant contribution but is slightly red shifted (see Fig. 1c). Therefore, it is assigned to energy redistribution processes, *e.g.* charge localisation in the ligand, which cause a blue shift of the TA spectra.

With this interpretation and literature precedent,[15–17,35] the DAS within the first few picoseconds are assigned to the ^{3}MLCT state of $\mathbf{1}^{2+}$. Intersystem crossing from ^{1}MLCT to ^{3}MLCT is faster than the time resolution of our instrument (<100 fs). Based on the observed decay of the TA spectra, relaxation of the ^{3}MLCT state back to the ground state occurs either directly or *via* an intermediate state that is only transiently populated and thus not observed. Typically, ^{3}MC and ^{5}MC states serve as deactivating pathways for iron(II) complexes.[5–8] Iron(II) complexes with the ^{5}MC state as lowest excited state possess high ^{5}MC lifetimes up to several nanoseconds, for example the $^5T_2$–$^1A_1$ ground state recovery time of $[Fe(tpy)_2]^{2+}$ is 4 ns.[36,37] On the other hand, complexes with the ^{3}MC state lower than the ^{5}MC state possess ^{3}MC lifetimes of only a few ps and sometimes even less. For example, $[Fe(CNC)_2]^{2+}$ complexes with methyl and isopropyl N-substituents show ^{3}MC lifetimes <2 ps and <8 ps, significantly shorter than the ^{3}MLCT lifetime.[16,17] A similar situation might be operative in $\mathbf{1}^{2+}$ with only two carbene ligands: the ^{5}MC state is higher in energy than the ^{3}MC state which decays rapidly to the ground state and is consequently not observed, similar to $[Fe(CNC)_2]^{2+}$.[19]

To substantiate this interpretation, the lowest triplet and quintet MC states of $\mathbf{1}^{2+}$ were calculated by DFT (Fig. 2). The ^{3}MC state is slightly lower in energy than the ^{5}MC state. In the triplet state, the two Fe–N distances of the *trans* positioned pyridines are strongly elongated from 2.013/2.015 Å to 2.348/2.358 Å, while the other Fe–C/N distances are hardly affected. This is consistent with the population of the d_z^2 orbital with the

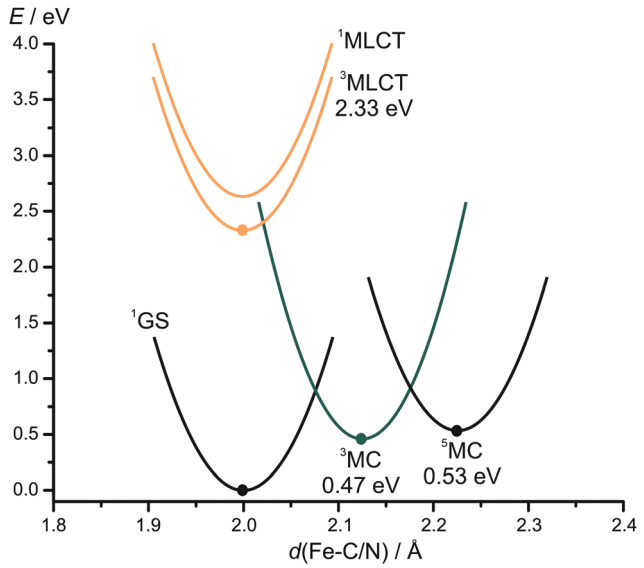

Fig. 2 Summary of the quantum chemically calculated energetics of $\mathbf{1}^{2+}$ as obtained from DFT calculations (•) or experimental data (^{1}MLCT), with parabolic energy surfaces sketched qualitatively as visual guides for discussion purposes.

z-axis experiencing the weakest ligand field strength. In the ^{5}MC high spin-state, all Fe–C/N distances are elongated due to the population of the d_z^2 and $d_{x^2-y^2}$ orbitals. The large distortions impose a reorganisation barrier between the nearly degenerate ^{3}MC and ^{5}MC states. This substantiates the interpretation that the ^{5}MC state is by-passed and that the ^{3}MC state undergoes ISC to the ground state. Attempts to optimise the ^{3}MLCT state by DFT without constraints were unsuccessful as all optimisation attempts converged to the ^{3}MC state. By constraining all Fe–C/N bond distances to 1.9 Å, convergence to a ^{3}MLCT state with spin density at the iron and a pyridine ring and an energy of 2.33 eV (532 nm) was achieved. This estimated ^{3}MLCT energy is consistent with the experimental ^{1}MLCT state energy of 2.48 eV (500 nm). Assuming that all MLCT states are rather nested with the ground state,[19] population transfer from the $^{1/3}$MLCT states to the ^{3}MC state is burdened with a reorganisation energy. In combination with the comparably high ^{3}MC energy, this barrier accounts for the high ^{3}MLCT lifetime of $\mathbf{1}^{2+}$ of 9.2 ps. Such a high lifetime of a ^{3}MLCT state in iron(II) complexes has been only realised so far using four carbene donors instead of only two in $\mathbf{1}^{2+}$.[16,17]

Emission from the ^{3}MLCT state after excitation of $\mathbf{1}^{2+}$ at 413 or 500 nm at room temperature in MeCN or at 77 K in a frozen ^{n}PrCN glass was not observed indicating that the ^{3}MLCT–^{3}MC barrier can efficiently be overcome even at 77 K.

Carbenes also stabilise low-spin iron(III) and ^{2}LMCT states of iron(III) complexes can be photoactive.[30,38] Consequently, emission of the iron(III) complex $\mathbf{1}^{3+}$, prepared *in situ* by oxidation of $\mathbf{1}^{2+}$ with [NO][PF_6], was probed by exciting at 524 and 609 nm at room temperature and at 77 K. However, no ^{2}LMCT fluorescence of $\mathbf{1}^{3+}$ was detected with our instrument.

The iron(II) complex $[Fe(dpmi)_2]^{2+}$ $\mathbf{1}^{2+}$ with a two carbene/four pyridine [C_2N_4] donor set and a high octahedral symmetry enabled by six-membered chelate rings in a rigid environment

exhibits a high ^{3}MLCT lifetime of 9.2 ps. This value compares to lifetimes of iron(II) complexes with a four carbene/two pyridine [C_4N_2] donor set in a more distorted environment with five-membered chelate rings. This observation validates the high symmetry concept to increase the energy of MC states by a better metal–ligand orbital overlap. Deactivation of the ^{3}MLCT state of $\mathbf{1}^{2+}$ likely occurs *via* the tetragonally distorted ^{3}MC state by-passing the ^{5}MC state resembling the photodynamics of classical polypyridine ruthenium(II) complexes.[19] The combination of six-membered chelates and strong σ-donating carbenes paves the way to photoactive, luminescent and solar energy-converting iron(II) complexes with long ^{3}MLCT lifetimes. A future challenge will be the increasingly facile Fe^{II}/Fe^{III} oxidation with a high number of carbene donors and the smaller MLCT extinction coefficient in all-carbene complexes lacking π-accepting ligands.[20,30,37]

TR performed the synthesis, ground state characterisation and the DFT calculations. AK and SL measured and interpreted the TA data. RS and MB measured and interpreted the XAS data. KH designed and supervised the project, analysed the data and wrote the manuscript.

Financial support from the Deutsche Forschungsgemeinschaft [Priority Program SPP 2102 ''Light-controlled reactivity of metal complexes'' (HE 2778/14-1, BA 4467/7-1, LO 714/11-1)] is gratefully acknowledged. Parts of this research were conducted using the supercomputers MOGON and Elwetritsch and advisory services offered by Johannes Gutenberg university Mainz (http://www.hpc.uni-mainz.de) and TU Kaiserslautern (https://elwe.rhrk.uni-kl.de), which are members of the AHRP. PETRA III is kindly acknowledged for provision of beamtime at beamline P65.

Conflicts of interest

There are no conflicts to declare.

Notes and references

1 C. Förster and K. Heinze, *Chem. Soc. Rev.*, 2020, **49**, 1057.
2 O. S. Wenger, *J. Am. Chem. Soc.*, 2018, **140**(42), 13522.
3 C. Bizzarri, E. Spuling, D. M. Knoll, D. Volz and S. Bräse, *Coord. Chem. Rev.*, 2018, **373**, 49.
4 B. M. Hockin, C. Li, N. Robertson and E. Zysman-Colman, *Catal. Sci. Technol.*, 2019, **9**, 889.
5 O. S. Wenger, *Chem. – Eur. J.*, 2019, **25**, 6043.
6 Y. Liu, P. Persson, V. Sundström and K. Wärnmark, *Acc. Chem. Res.*, 2016, **49**, 1477.
7 S. Kaufhold and K. Wärnmark, *Catalysts*, 2020, **10**, 132.
8 B. C. Paulus, S. L. Adelman, L. L. Jamula and J. K. McCusker, *Nature*, 2020, **582**, 214.
9 J. K. McCusker, *Science*, 2019, **363**, 484.
10 S. Campagna, F. Puntoriero, F. Nastasi, G. Bergamini and V. Balzani, Photochemistry and Photophysics of Coordination Compounds: ruthenium, *Topics in Current Chemistry*, Springer, Berlin, Heidelberg, 2007, vol. 280, p. 117.
11 L. Flamigni, A. Barbieri, C. Sabatini, B. Ventura and F. Barigelletti, Photochemistry and Photophysics of Coordination Compounds: iridium, *Topics in Current Chemistry*, Springer, Berlin, Heidelberg, 2007, vol. 281, p. 143.
12 L. L. Jamula, A. M. Brown, D. Guo and J. K. McCusker, *Inorg. Chem.*, 2014, **53**, 15.
13 A. K. C. Mengel, C. Förster, A. Breivogel, K. Mack, J. R. Ochsmann, F. Laquai, V. Ksenofontov and K. Heinze, *Chem. – Eur. J.*, 2015, **21**, 704.
14 A. K. C. Mengel, C. Bissinger, M. Dorn, O. Back, C. Förster and K. Heinze, *Chem. – Eur. J.*, 2017, **23**, 7920.
15 M. Darari, E. Domenichini, A. Francés-Monerris, C. Cebrián, K. Magra, M. Beley, M. Pastore, A. Monari, X. Assfeld, S. Haacke and P. C. Gros, *Dalton Trans.*, 2019, **48**, 10915.
16 Y. Liu, T. C. B. Harlang, S. E. Canton, P. Chábera, K. Suárez-Alcántara, A. Fleckhaus, D. A. Vithanage, E. Göransson, A. Corani, R. Lomoth, V. Sundström and K. Wärnmark, *Chem. Commun.*, 2013, **49**, 6412.
17 P. Zimmer, L. Burkhardt, A. Friedrich, J. Steube, A. Neuba, R. Schepper, P. Müller, U. Flörke, M. Huber, S. Lochbrunner and M. Bauer, *Inorg. Chem.*, 2018, **57**, 360.
18 T. Harlang, Y. Liu, O. Gordivska, L. Fredin, C. Ponseca Jr., P. Huang, P. Chábera, K. Kjær, H. Mateos, J. Uhlig, R. Lomoth, R. Wallenberg, S. Styring, P. Perrson, V. Sundström and K. Wärnmark, *Nat. Chem.*, 2015, **7**, 883.
19 L. A. Fredin, M. Pápai, E. Rozsályi, G. Vanko, K. Wärnmark, V. Sundström and P. Persson, *J. Phys. Chem. Lett.*, 2014, **5**, 2066.
20 P. Chábera, K. Kjær, O. Prakash, A. Honarfar, Y. Liu, L. Fredin, T. Harlang, S. Lidin, J. Uhlig, V. Sundström, R. Lomoth, P. Perrson and K. Wärnmark, *J. Phys. Chem. Lett.*, 2018, **9**, 459.
21 M. Abrahamsson, M. Jäger, T. Österman, L. Eriksson, P. Persson, H.-C. Becker, O. Johansson and L. Hammarström, *J. Am. Chem. Soc.*, 2006, **128**, 12616.
22 M. Abrahamsson, H.-C. Becker, L. Hammarström, C. Bonnefous, C. Chamchoumis and R. P. Thummel, *Inorg. Chem.*, 2007, **46**, 10354.
23 M. Abrahamsson, M. Jäger, R. J. Kumar, T. Österman, P. Persson, H.-C. Becker, O. Johansson and L. Hammarström, *J. Am. Chem. Soc.*, 2008, **130**, 15533.
24 A. Breivogel, C. Förster and K. Heinze, *Inorg. Chem.*, 2010, **49**, 7052.
25 A. Breivogel, M. Meister, C. Förster, F. Laquai and K. Heinze, *Chem. – Eur. J.*, 2013, **19**, 13745.
26 M. Dorn, J. Kalmbach, P. Boden, A. Päpcke, S. Gómez, C. Förster, F. Kuczelinis, L. M. Carrella, L. Büldt, N. Bings, E. Rentschler, S. Lochbrunner, L. González, M. Gerhards, M. Seitz and K. Heinze, *J. Am. Chem. Soc.*, 2020, **142**, 7947.
27 S. Treiling, C. Wang, C. Förster, F. Reichenauer, J. Kalmbach, P. Boden, J. P. Harris, L. Carrella, E. Rentschler, U. Resch-Genger, C. Reber, M. Seitz, M. Gerhards and K. Heinze, *Angew. Chem., Int. Ed.*, 2019, **58**, 18075.
28 S. Otto, M. Grabolle, C. Förster, C. Kreitner, U. Resch-Genger and K. Heinze, *Angew. Chem., Int. Ed.*, 2015, **54**, 11572.
29 J. P. Harris, C. Reber, H. E. Colmer, T. A. Jackson, A. P. Forshaw, J. M. Smith, R. A. Kinney and J. Telser, *Can. J. Chem.*, 2020, **98**, 250.
30 K. S. Kjær, N. Kaul, O. Prakash, P. Chábera, N. W. Rosemann, A. Honarfar, O. Gordivska, L. A. Fredin, K.-E. Bergquist, L. Häggström, T. Ericsson, L. Lindh, A. Yartsev, S. Styring, P. Huang, J. Uhlig, J. Bendix, D. Strand, V. Sundström, P. Persson, R. Lomoth and K. Wärnmark, *Science*, 2019, **363**, 249.
31 M. Darari, A. Francés-Monerris, B. Marekha, A. Doudouh, E. Wenger, A. Monari, S. Haacke and P. C. Gros, *Molecules*, 2020, **25**, 5991.
32 V. Tran, K. E. Allen, M. Garcia Chavez, C. Aaron, J. J. Dumais, J. T. York and E. C. Brown, *Polyhedron*, 2018, **147**, 131.
33 G. Vankó, T. Neisius, G. Molnár, F. Renz, S. Kárpáti, A. Shukla and F. M. F. de Groot, *J. Phys. Chem. B*, 2006, **110**, 11647.
34 F. Plasser, *J. Chem. Phys.*, 2020, **152**, 084108.
35 A. M. Brown, C. E. McCusker and J. K. McCusker, *Dalton Trans.*, 2014, **43**, 17635.
36 J. K. McCusker, A. L. Rheingold and D. N. Hendrickson, *Inorg. Chem.*, 1996, **35**, 2100.
37 A. Hauser, C. Enachescu, M. L. Daku, A. Vargas and N. Amstutz, *Coord. Chem. Rev.*, 2006, **250**, 1642.
38 P. Chábera, Y. Liu, O. Prakash, E. Thyrhaug, A. El Nahhas, A. Honarfar, S. Essén, L. A. Fredin, T. C. B. Harlang, K. S. Kjær, K. Handrup, F. Ericson, H. Tatsuno, K. Morgan, J. Schnadt, L. Häggström, T. Ericsson, A. Sobkowiak, S. Lidin, P. Huang, S. Styring, J. Uhlig, J. Bendix, R. Lomoth, V. Sundström, P. Persson and K. Wärnmark, *Nature*, 2017, **543**, 695.

